Available online at www.sciencedirect.com
SCIENCE DIRECT®
Journal of Chromatography A, 984 (2003) 67–79
JOURNAL OF CHROMATOGRAPHY A
www.elsevier.com/locate/chroma

Practical implications of ionic strength effects on particle retention in thermal field-flow fractionation

Paul M. Shiundu[a,*], Stephen M. Munguti[a], S. Kim Ratanathanawongs Williams[b]

[a]*Department of Chemistry, University of Nairobi, P.O. Box 30197, Nairobi, Kenya*
[b]*Department of Chemistry and Geochemistry, Colorado School of Mines, 1500 Illinois Street, Golden, CO 80401, USA*

Received 17 July 2002; received in revised form 22 October 2002; accepted 24 October 2002

Abstract

Modification of ionic strength of an aqueous or non-aqueous carrier solution can have profound effects on the particle retention behavior in thermal field-flow fractionation (ThFFF). These effects can be considered as either advantageous or not depending on the performance criteria under consideration. Aside from the general increase in retention time of particulate material (latexes and silica particles), our experiments indicate improvement in resolution with increases in electrolyte concentration. Absence of an electrolyte in the carrier solution causes deviations from the theoretically expected linear behavior between the retention parameter λ (a measure of the extent of interaction between the applied field and the particle) and the reciprocal temperature drop across the channel walls. A negative interaction parameter δ_w of about -0.170 was determined for 0.105- and 0.220-μm polystyrene (PS) latex particles suspended in either a 0.25 or a 1.0 m*M* TBAP-containing acetonitrile carrier and for 0.220 μm PS in 0.50 and 1.0 m*M* NaCl-containing aqueous medium. This work also demonstrates that optimum electrolyte concentrations can be chosen to achieve reasonable experimental run-times, good resolution separations, and shifts in the steric inversion points at lower field strengths, and that too high electrolyte concentrations can have deleterious effects such as band broadening and sample loss through adsorption to the channel accumulation surface. The advantages of using ionic strength rather than field strength to effect desired changes are lowered power consumption and possible application of ThFFF to high temperature-labile samples.

Keywords: Thermal field-flow fractionation; Ionic strength; Interaction parameter; Particle retention; Field-flow fractionation; Steric inversion diameter; Diameter-based selectivity

1. Introduction

Field-flow fractionation (FFF) is a family of chromatography-like techniques in which an externally applied field or gradient acts on a sample in a direction perpendicular to the flow axis in an open thin ribbon-like channel [1–3]. The techniques have been used successfully to separate and characterize a broad range of macromolecular, colloidal, and particulate materials [1]. Field-flow fractionation has the capability for measuring numerous properties of macromolecular and colloidal particles, including particle mass (molecular mass), size, density, porosity, charge, diffusivity, and thermal diffusion coefficients [1,4,5]. This capability arises from the physical simplicity of the thin FFF separation channel and the resultant simplicity of retention theory

*Corresponding author. Fax: +254-2-446138.
E-mail address: pmshiundu@uonbi.ac.ke (P.M. Shiundu).

0021-9673/02/$ – see front matter
PII: S0021-9673(02)01769-7

which connects measurable retention time t_r for the component of interest to its properties.

For the FFF technique known as thermal FFF (ThFFF), the external field is a temperature gradient, which forces the sample components toward one of the channel walls (normally referred to as the accumulation wall) by the process of thermal diffusion (or thermophoresis) [6]. Since its inception (nearly four decades ago), ThFFF has been predominantly used for the separation and characterization of synthetic polymers [7–19]. However, during the past decade, ThFFF has been successfully applied to the retention and fractionation of colloids and particles suspended in both aqueous and non-aqueous carrier liquids [20–27]. In ThFFF, particles are separated selectively according to size in both the colloidal range (those under 1 μm diameter) and the micrometer-size range. Retention of particles in ThFFF has also been found to be composition-dependent [23–26], and this presents unique opportunities for the separation and characterization of complex materials. An apparent sensitivity of the retention of colloidal particles on the composition of particle surface has also been demonstrated [23–25] thereby showing the potential of ThFFF to determine the chemical composition of particle surfaces. The dual size–composition dependence of retention in ThFFF has the potential to provide particle compositional analysis.

Retention dependence on chemical composition in ThFFF is however, not limited to particulate materials. Earlier studies with polymers have shown that retention in ThFFF is not only dependent on polymer molecular mass but also on the polymer chemical composition [17–19]. However, in order to take advantage of the opportunities presented by this retention dependence on chemical composition phenomenon in ThFFF, it has been recognized by various workers that a better understanding of the thermal diffusion phenomenon (the phenomenon governing retention in ThFFF) is a necessity. A comprehension of the exact nature of the influence that chemical composition as well as other parameters associated with polymeric and particulate matter have on the thermal diffusion coefficient, would be ideal. Driven by this need to better understand the factors that influence D_T, various workers have carried out a series of empirical studies, which have provided important trends [20–27]. For instance, it is now clear that D_T is sensitive not only to the chemical nature of the suspended material but also to the composition of the carrier liquid [22,25,27]. It is significant to note that ThFFF has also been used to accumulate data on the compositional dependence of D_T for both dissolved and suspended matter.

From the standard retention theory of FFF [1], expressions that relate experimentally measured retention times with various physicochemical parameters of sample analyte have been successfully developed for each type of field. While these expressions are sufficiently rigorous, retention perturbations arising from various factors have been found to introduce errors in colloidal and macromolecular properties measured by FFF techniques [28] and by extension to D_T calculations. Giddings [28] divided the measurement errors into two categories: those arising from shortcomings in the theoretical retention models that allow properties to be deduced from measured retention times and those from experimental errors in retention time measurements and in system parameters that enter the final calculations of properties. These errors have been attributed to several assumptions in the standard FFF retention theory [28] and include the assumed parabolic flow between the planar walls, non-interacting sample particles, uniform field-induced forces across the channel, and absence of extraneous non-uniform forces acting transversely between the channel walls [29].

Several authors have reported perturbations on the retention behavior of particles suspended in low ionic strength carrier solutions in sedimentation FFF (SdFFF) [29–33]. Hansen et al. [29,30] and Mori et al. [31] attributed the perturbations in SdFFF to particle–wall and particle–particle interactions. Tekeuchi et al. [33] explained the dependence of retention on the type and concentration of surfactant added to an eluant on a small deviation from the parabolic flow profile in the region near the channel wall. These observations however, are not unique to SdFFF. Perturbations on ThFFF retention of particles arising from ionic strength modification of carrier solutions have been observed and explanations offered by various researchers [21,22,25,27,34,35]. Despite these apparent perturbations to the retention of particles in a ThFFF channel, the potential practi-

cal benefits of ionic strength effects to the utility of ThFFF as a viable technique for colloidal and particle retention and separation system has not been sufficiently highlighted or explored.

In this paper, we demonstrate the potential opportunities and limitations that variation of carrier ionic strength can have on the practical utility of ThFFF for particle separation and characterization. The primary goal of this work is to provide further insight into the behavior of colloids and particles in ionic strength modified carrier solutions (aqueous and non-aqueous) in a ThFFF system. This work is unique in that it focuses on the exploitation of carrier solution ionic strength in the development of ThFFF as a particle separation and characterization technique.

2. Theory of ThFFF

Sample components introduced into an FFF channel interact with the externally applied field, which forces them to migrate transversely across the channel towards the accumulation wall. How far a sample component is moved towards the accumulation wall will depend on the extent of interaction between the applied field and the component. This is the origin of differential migration since different sample components experience different magnitudes of forces, which compresses them into layers of different thicknesses against the accumulation wall. In the normal mode of operation [36], the resulting compression of sample components in the direction of the applied field is opposed by ordinary mass diffusion, leading to a concentration profile that decreases exponentially with distance from the accumulation wall. Ordinarily, each sample component forms a distinct concentration profile, which is characteristic of its extent of interaction with the applied field. The concentration profile can be characterized by a distance, l between the cloud's center of gravity and the accumulation wall. When a parabolic flow displaces an exponential component cloud, the retention time t_r, can be represented by the standard retention equation [37]:

$$t_r = \frac{t^0}{6\lambda\left[\coth\left(\frac{1}{2\lambda} - 2\lambda\right)\right]} \quad (1)$$

where λ ($=l/w$) is a dimensionless retention parameter, w is the FFF channel thickness and t^0 is the time needed to elute a non-retained component from the FFF channel. With an approximately parabolic flow profile across the channel thickness, the liquid carrier velocity increases away from the accumulation wall towards the center of the channel. The retention parameter λ can be considered as a measure of the extent of interaction between the sample component and the externally applied field. Sample components that interact strongly with the applied field get pushed closer to the accumulation wall and thereby have a smaller λ.

For ThFFF, λ is related to two transport processes of ordinary (mass) diffusion coefficient D and thermal diffusion coefficient D_T by the expression:

$$\lambda = \frac{D}{D_T \Delta T} \quad (2)$$

where ΔT is the temperature drop across the hot and cold walls of the ThFFF channel system. In ThFFF, Eq. (1) is normally corrected for perturbations in the flow profile within the channel brought about by the temperature–viscosity variations arising from the temperature gradient across the channel [38]. This correction becomes particularly significant when calculating sample-solution parameters such as D_T from the experimentally measured t_r values.

For highly retained sample components (i.e. $\lambda \rightarrow 0$), the following limiting form of Eq. (1) is used.

$$\frac{t_r}{t^0} = \frac{1}{6\lambda} \quad (3)$$

Combining Eqs. (2) and (3), we obtain:

$$\frac{t_r}{t^0} = \frac{D_T \Delta T}{6D} = \left(\frac{D_T}{D}\right) \cdot \left(\frac{\Delta T}{6}\right) \quad (4)$$

It is evident from Eq. (4) that at constant ΔT, variations in experimentally determined retention time t_r originate from differences in the ratio D_T/D. This implies that for components having the same D values (i.e. components having the same hydrodynamic size), differences in t_r at constant ΔT can only be attributed to variations in their D_T values.

Using the Stokes–Einstein equation in which:

$$D = \frac{kT}{3\pi\eta d} \tag{5}$$

where d is the hydrodynamic diameter of a molecule or particle, k is the Boltzmann constant, T is absolute temperature, and η is the viscosity of the carrier liquid, Eq. (4) can be re-expressed as:

$$\frac{t_r}{t^0} = \frac{\pi\eta d\Delta T D_T}{2kT} \tag{6}$$

Here too, it can be seen that other than d and ΔT, D_T (and by extension any other factors affecting it) is the retention time-controlling parameter in ThFFF for a given carrier solution.

The ability to differentially retain and therefore resolve particles of different sizes is related to the diameter-based selectivity S_d that can be defined as [20]:

$$S_d = \frac{d \log\left(\frac{t_r}{t^0}\right)}{d \log d} \tag{7}$$

If we assume that the only parameters in Eq. (6) that depend on particle diameter are d and D_T, substituting the expression for t_r/t^0 of Eq. (6) into Eq. (7) yields:

$$S_d = 1 + \frac{d \log D_T}{d \log d} \tag{8}$$

The S_d value for particles of a given composition can therefore be obtained from the slopes of the log (t_r/t^0) versus log d plots.

3. Experimental

The ThFFF instrument used in this work is similar in design to the Model T100 Polymer fractionator from FFFractionation Inc. (now PostNova Analytics, Salt Lake City, UT, USA). A 76-μm (or 114-μm) Mylar channel spacer was confined between two chrome-plated copper bars, with the top bar heated using rods controlled by relay switches with cycle times activated by a microprocessor. The cold wall was cooled using continuously flowing tap water. The temperatures of the hot and cold walls were monitored through three sensors that were inserted (two in the hot and one in the cold wall) into wells drilled into both the top and bottom bars.

The channel cut out of the 76-μm Mylar spacer had a tip-to-tip length of 46 cm and a breadth of 2.0 cm with a resultant void volume of 0.58 ml. Carrier liquids were prepared from either deionized water or Spectrograde acetonitrile (ACN) obtained from EM Science (Cherry Hill, NJ, USA). The carrier liquids were delivered using a Model M-6000A pump from Waters Associates (Milford, MA, USA). The ionic strength of ACN was modified to varying extents using different appropriate weights of tetrabutylammonium perchlorate (TBAP), whereas that of the aqueous carrier was modified using either analytical grade sodium chloride or sodium azide. In other circumstances, the aqueous carrier consisted of doubly distilled water containing 0.1% FL-70 surfactant plus 0.02% sodium azide. A model UV-106 detector from Cole Scientific (Calasabas, CA, USA) operating at 254 nm wavelength was used to detect particles eluting from the ThFFF channel. Data acquisition of the detector signal was made using a PC-AT compatible computer. The hardcopy of the detector signal was also recorded using an OmniScribe chart recorder from Houston Instruments (Austin, TX, USA). Samples were injected via a 20-μl loop injection valve.

Standard polystyrene (PS) latex beads of diameters 0.105, 0.220, 0.222, 0.280, 0.300, 0.398, 0.426, 0.598, 1.05, 1.48, 1.75, 2.08, 3.00, 3.98, 5.01, 8.7, 9.87, and 15.00 μm used in this work were obtained from Duke Scientific (Palo Alto, CA, USA). Silica particles of diameter 0.25 μm were obtained from Merck (Darmstadt, Germany).

4. Results and discussion

The standard FFF retention theory given in Eq. (1) assumes the absence of extraneous nonuniform forces acting transversely between FFF channel walls among other assumptions. Thus, λ should vary linearly with $1/\Delta T$ as exemplified by Eq. (2) and pass through the origin. Fig. 1 shows plots of λ versus $1/\Delta T$ for both 0.105- and 0.220-μm PS particles in ACN carrier solution containing different concentrations of TBAP. It is clearly evident from the figure that the plots corresponding to TBAP-

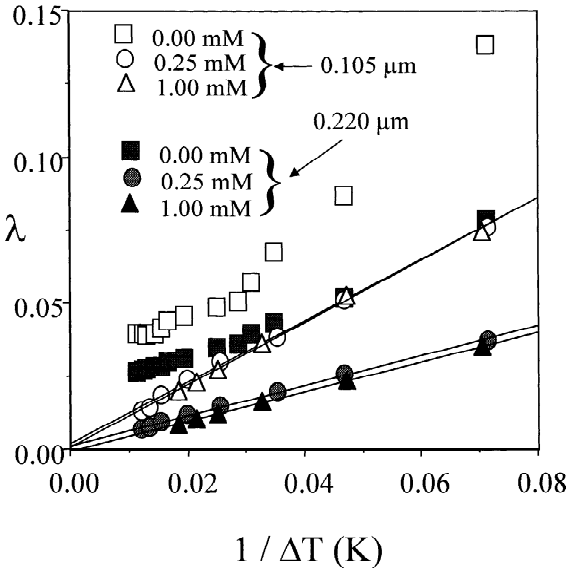

Fig. 1. Plots of λ versus $1/\Delta T$ for 0.105-μm (open symbols) and 0.220-μm (filled symbols) PS latex particles with ACN carrier liquid in the absence and presence of various concentrations of TBAP. Experimental conditions: flow-rate = 0.30 ml/min and w = 76 μm.

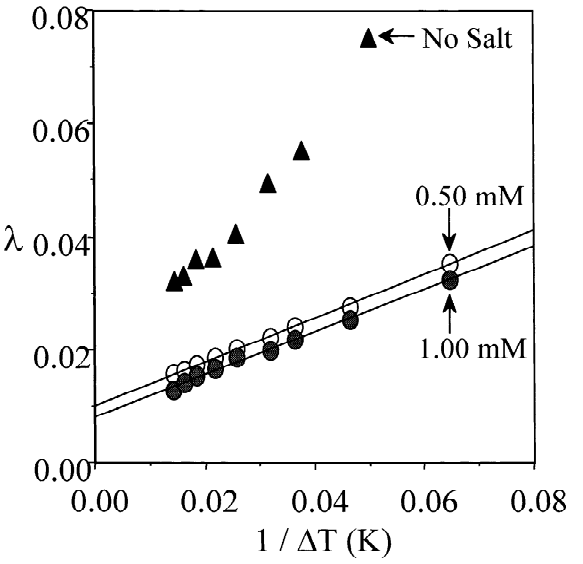

Fig. 2. Plots of λ versus $1/\Delta T$ for 0.220-μm PS latex particles with an aqueous carrier liquid in the absence and presence of 0.50 and 1.00 mM concentrations of NaCl. Experimental conditions: flow-rate = 0.30 ml/min and w = 76 μm.

containing carriers are linear and intercept the ordinate at a value of zero (within experimental error) unlike their TBAP-free counterparts. The TBAP-free plots indicate that the λ values corresponding to smaller $1/\Delta T$ values (i.e. larger ΔT values) are larger than they should be and hence the pronounced deviation from the expected linearity.

Similar linear and non-linear plots of λ versus $1/\Delta T$ were obtained for 0.220-μm PS particles suspended in NaCl-containing (0.50 or 1.00 mM) and NaCl-free aqueous carriers, respectively, and the results are displayed in Fig. 2. It is significant that the linear plots for the aqueous carrier do not however, intercept the ordinate at a value of zero as is the case with ACN carrier of Fig. 1. The noticeable trend of increasing retention (i.e. smaller λ values) of the latex particles when TBAP is added to ACN carrier or when NaCl is added to the aqueous carrier is consistent with previous reports [22,25–27]. There is increasing evidence that thermal diffusion (the driving force behind retention in ThFFF) is dominated by surface effects [23,39,40] and that the retention of particles in ThFFF is significantly influenced by ionic strength of the carrier liquid [21,22,25,27]. Whereas an earlier report [22] attributed ionic strength effects purely to electrostatic phenomena, recent studies have cited surface tension as the dominant factor, particularly for latex particles [25,26,34]. Jeon and Schimpf [26] report that the increase in retention of latex particles with NaN_3 concentration is consistent with an increase in thermal diffusion with surface tension, since surface tension increases with salt concentration. They report that electrostatic effects on particle retention are due to either particle–wall interactions or actual changes in thermophoresis. The concept behind particle–wall interactions is that as the double layers of two surfaces of similar charge overlap, the surfaces repel one another. Thus, the electrostatic repulsion of particles from the accumulation wall of a ThFFF system forces particles into the faster-moving flow streamlines located away from the wall, thereby decreasing particle retention. This would explain the reduced retention of the PS particles in either TBAP-free ACN or NaCl-free aqueous carriers (shown in Figs. 1 and 2) and probably account for the non-linearity in the corresponding plots of λ versus $1/\Delta T$. The reasoning is that as the ionic strength of the carrier solutions is increased, the thickness of the

corresponding double layers decreases [31], therefore retention of the PS particles in the electrolyte-containing carrier increases as is evident from the two figures. However, besides the repulsive type interactions, one can also expect attractive particle–wall interactions of the London-van der Waals type [29] to dominate at high enough ionic strength [31].

From the foregoing section, it is clear that both electrostatic and surface tension phenomena can be at play in determining the retention of particles in ThFFF. Thus, it will be important to differentiate the contribution of thermal diffusion from that of electrostatic interactions in particle retention. We therefore examine our data for possible particle–wall interactions by employing the semiempirical interaction parameter δ_w, introduced by Williams et al. [41]. The interaction parameter is defined as:

$$\delta_w = \int_0^\infty \{1 - \exp[-V_w(\delta)/kT]\}\mathrm{d}\delta \quad (9)$$

where δ is the distance from the particle surface to the accumulation wall and V_w is the energy of interaction between the particle and the wall as a function of the distance between them. The parameter δ_w will be positive for a dominant repulsive interaction and negative for a net attraction. The distance δ_w will be independent of field strength applied provided the particle interaction with the wall varies sufficiently rapidly. According to Williams et al. [41], δ_w is likely to be dependent on particle and wall compositions, surface properties, composition of the carrier fluid and/or particle size. The value of δ_w is obtained by measuring the retention of a given particle over a range of field strengths and plotting the function:

$$f(R,\alpha,\lambda) = \frac{R_p - 6\alpha(1-\alpha)}{6\lambda\{(1-2\alpha)\coth[(1-2\alpha)/2\lambda] - 2\lambda\}} = 1 + \frac{\delta_w}{\ell} \quad (10)$$

where R_p is the retention ratio perturbed by the particle–wall interaction, λ is defined by Eq. (2), α is the ratio of the particle radius to the channel thickness w and $l = w\lambda$. A plot of $f(R,\alpha,\lambda)$ versus $1/l$ yields a slope equal to δ_w and an intercept of unity.

Fig. 3 displays the plots of $f(R,\alpha,\lambda)$ versus $1/l$ for

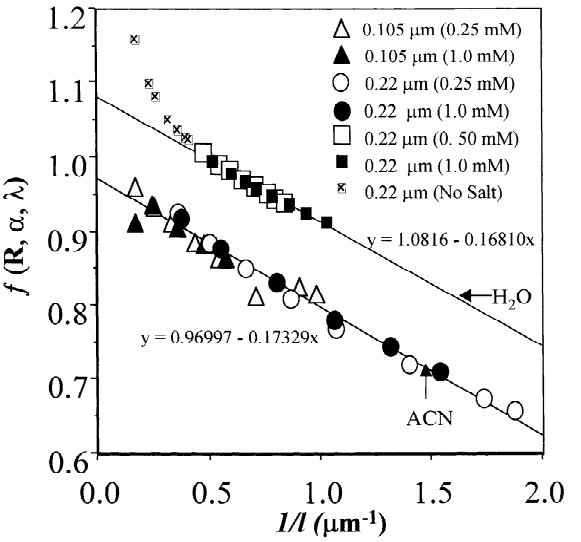

Fig. 3. Retention data for 0.105- and 0.220-μm PS particles in TBAP-containing ACN carrier and 0.220-μm PS particles in aqueous carrier (containing 0.0, 0.50 or 1.0 m*M* NaCl) measured at a channel flow-rate of 0.30 ml/min, plotted in the form of $f(R,\alpha,\lambda)$ versus $1/l$. The different symbols represent data for 0.105- or 0.220-μm PS particles suspended in either ACN or aqueous carriers containing different concentrations of either TBAP or NaCl, respectively.

data represented in Fig. 1 for 0.105 and 0.220 μm PS (except data obtained in the TBAP-free ACN) and data for 0.220 μm PS latex particles of Fig. 2. The ΔT-values used ranged from 14 to 83 K and from 20 to 70 K for ACN and H_2O carriers, respectively. There are several features in the plots of Fig. 3 worth noting: (1) To a good approximation, the data (with ACN as carrier) for the 0.105 and 0.220 μm PS particles in both 0.25 and 1.0 m*M* NaCl concentration appear to fall on a common straight line with an intercept (0.970) close to unity and a negative slope (δ_w) equal to −0.173. (2) The data for 0.220 μm PS in NaCl-containing aqueous carrier fall on a common straight line with an intercept (1.082) also close to unity (but slightly larger than that in ACN) and a negative slope of −0.168. (3) The plots for the two carrier systems are nearly parallel to each other (i.e. the slopes can be said to be similar within good approximation). (4) The plots obtained in the NaCl-free aqueous carrier exhibit curvature in the region of high $f(R,\alpha,\lambda)$ values (or low $1/l$ values) which correspond to reduced retention of the 0.220 μm PS

particles. From these observations, some general conclusions can be made. (1) That for this particular combination of accumulation wall (chrome-plated copper bar), carrier solutions (ACN–TBAP and H_2O–NaCl), particle material and the range of ΔT values used, the δ_w parameter appears to be independent of the two particle sizes employed in the TBAP-containing ACN carrier and independent of NaCl concentration in the salt-containing aqueous media. (2) The negative value of δ_w (though small) is indicative of an attractive particle–wall electrostatic interaction under the NaCl and TBAP concentrations studied and that the particle cloud's center of gravity is closer to the wall than would be expected in the absence of the attractive particle–wall interactions. (3) The observed departure from linearity by the 0.220 μm PS particles in NaCl-free aqueous carrier can be attributed to their correspondingly low levels of retention as explained by Williams et al. [41]. According to Williams et al. [41], the presence of interactive forces having a lower dependence on δ (=to the distance between particle surface and the accumulation wall), will cause departures from the expected linearity of $f(R,\alpha,\lambda)$ versus $1/l$ plots. As a result, δ_w will tend to assume a dependence on field strength (in this case ΔT). The same argument holds for the nonlinear behavior observed for the PS particles in the TBAP-free ACN carrier. The established existence of an attractive particle–wall interaction supports our continuing observations of latex particle adsorption on a freshly cleaned chrome-plated ThFFF channel. This adsorption manifests as an absence of sample elution for the first several initial particle analyses in a newly assembled ThFFF channel with a freshly cleaned surface. This previously unreported observation with particles was believed to be associated with the initial channel surface coverage by the particles (a consequence of particle adsorption). Such adsorption processes become even more pronounced in the absence of a surfactant in the carrier liquid. As reported by Jeon et al. [25], absence of FL-70 surfactant in an aqueous carrier requires that samples be periodically sonicated to counteract their tendency to aggregate over time and also adsorb on a channel surface. The failure of the plots of λ versus $1/\Delta T$ data for PS in NaCl-containing aqueous carrier to intercept the ordinate at a value of zero (Fig. 2) is probably linked to their correspondingly larger than unity value of $f(R,\alpha,\lambda)$. This needs to be investigated further. While the δ_w values may shed some light on the nature of the interactions, they do not directly yield information on the extent of these interaction effects on particle retention, particularly in relation to D_T.

Using Eqs. (2) and (5) (after corrections for temperature and viscosity gradients across the channel [38]), ''apparent'' D_T values for various PS particle sizes were evaluated under different TBAP concentrations in ACN and the results are shown in Fig. 4. These D_T values were however, calculated without considering the potential effects of the electrical double layer on the hydrodynamic diameters of the various PS particles. The nominal diameters of the PS particles were used in the evaluation of the ordinary diffusion coefficient, D of Eq. (5). By neglecting the double layer thickness in estimating the hydrodynamic diameters of the particles, a biased D_T value could be obtained. Hence our use of the term ''apparent'' D_T. Unfortunately, the absence of appropriate data such as those of Figs. 1 and 2 under the TBAP concentrations given in Fig. 4 (for determination of the semiempirical interaction parame-

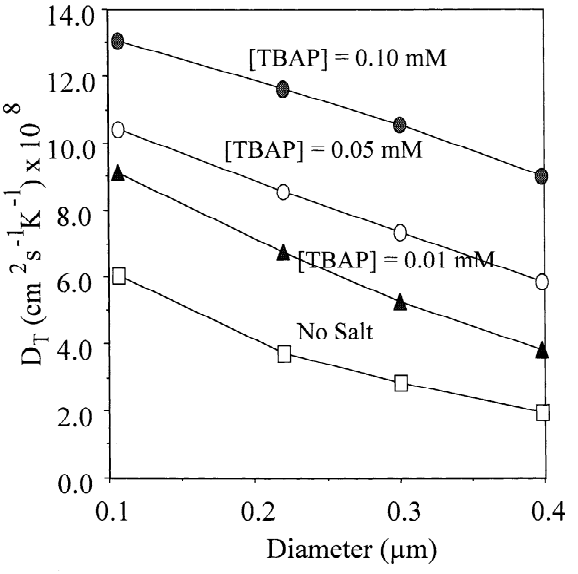

Fig. 4. Plots of D_T versus PS particle diameters (0.105, 0.220, 0.300 and 0.398 μm) in ACN carrier solution obtained for various concentrations of TBAP. Experimental conditions: flow-rate = 0.30 ml/min, ΔT = 40 K, T_c = 290 K and w = 76 μm.

ter δ_w) makes evaluation of the "true" D_T impossible. However, we expect the effect of the electrical double layer on the hydrodynamic diameters to be minor (particularly for the TBAP-containing carrier) due to the low electrical double layer expected in liquids of low dielectric constants such as ACN. Thus, the trends of D_T on particle size in ACN should be very close to that depicted in Fig. 4. More work however needs to be done to obtain the "true" D_T values.

The influence of NaN_3 concentration on inorganic particle retention was also investigated and the results are shown in Fig. 5a as superimposed elution profiles of 0.25-μm silica particles obtained under different concentrations of NaN_3 at a ΔT of 50 K. Here, the silica particle retention increases with NaN_3 concentration to a maximum retention time of about 25 min (measured at peak maximum) corresponding to a NaN_3 concentration of 18.50 m*M*. A higher NaN_3 concentration of 21.50 m*M* did not yield any further increase in the retention time for the silica particles but led to diminished peak intensity. Similar behavior in which the retention of latex particles in a FL-70-containing aqueous solution reaches a plateau as the NaN_3 concentration is increased has been reported by Jeon et al. [25]. However, the onset of the plateau was achieved at a concentration of approximately 30 m*M*. They also reported higher levels of retention of latex particles in FL-70-free aqueous carrier, but with diminished recoveries for NaN_3 concentrations above 5 m*M* and attributed this to sample adsorption to the accumulation wall. Our observation of reduced peak intensity for the silica particles at the NaN_3 concentration of 21.50 m*M* can also be attributed to sample adsorption to the channel surface (more evidence presented later). The difference in concentration of NaN_3 for the onset of adsorption is probably due to the lower thermophoretic mobilities of silica relative to latex particles [23] and differences in their surface charge densities. A corresponding plot of λ against concentration of NaN_3 for the 0.25-μm silica particles is given in Fig. 5b. From this figure, we can conclude that the distance of closest approach by the 0.25-μm silica particle to the accumulation wall when a ΔT of 50 K and a NaN_3 concentration of 18.5 m*M* are used is about 2 μm (equivalent to the mean layer thickness l of the sample cloud, since $\lambda = l/w$ and $w = 76$ μm).

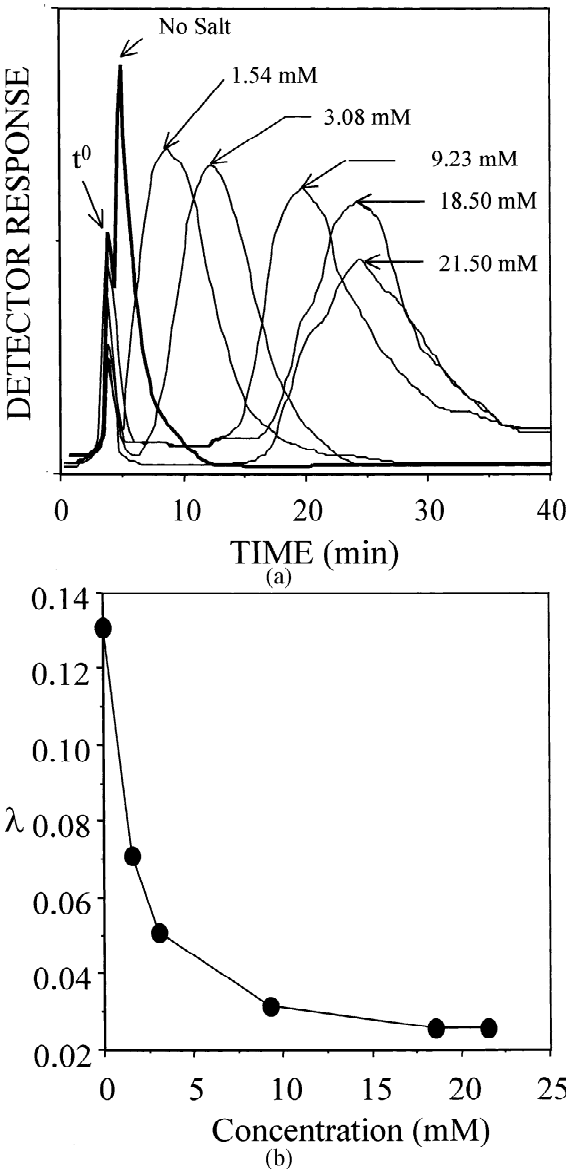

Fig. 5. (a) Superimposed elution profiles of 0.25-μm silica particles obtained under different concentration conditions of NaN_3 in aqueous carrier media. Experimental conditions: flow-rate = 0.30 ml/min, $\Delta T = 50$ K, $T_c = 298$ K and $w = 76$ μm. (b) Plot of λ versus concentration of NaN_3 for 0.25-μm silica particles in an aqueous carrier solution. Experimental conditions are the same as in (a).

Additional results showing the effect of various NaCl concentrations on the retention of different sizes of PS latex particles suspended in an aqueous carrier liquid are shown in Fig. 6. The figure

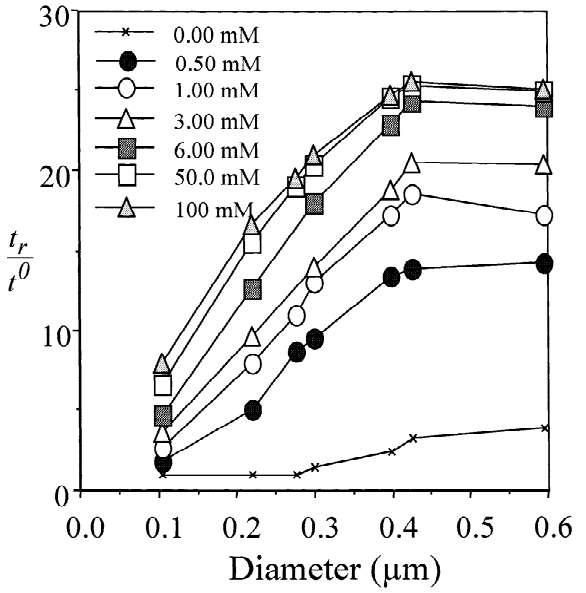

Fig. 6. Plots of t_r/t^0 versus PS latex particle diameters (0.105, 0.220, 0.280, 0.300, 0.398, 0.426 and 0.598 μm) obtained for various concentrations of NaCl in an aqueous carrier solution. Experimental conditions: flow-rate = 0.30 ml/min, $\Delta T = 50$ K, $T_c = 298$ K and $w = 76$ μm.

comprises plots of t_r/t^0 versus PS particle diameters obtained under different concentrations of NaCl. It is evident from the figure that below particle size of 0.42 μm, there is a general increase in slope of the t_r/t^0 versus diameter plot with increase in NaCl concentration. Beyond the 0.42-μm particle size, the t_r/t^0 versus diameter plots plateau off. This rather unusual behavior can be explained as a consequence of the phenomenon called steric inversion (see later).

The general increase in the slopes of the plots of t_r/t^0 versus diameter (with increases in concentration) indicates the practical utility of adding an electrolyte to a carrier solution to improve particle separation according to size by ThFFF. Fig. 7a shows the effect of NaN_3 concentration on the resolution between 0.105- and 0.220-μm PS particle sizes. In the absence of NaN_3, the resolution between the peaks is quite poor. However, the presence of 0.50 m*M* concentration of NaN_3 afforded baseline resolution between the peaks. In addition, the smaller 0.105-μm particle diameter is well resolved from the void peak. More elaborate studies showing the combined effects of TBAP concentration and ΔT on resolution are provided in Fig. 7b. This shows a plot

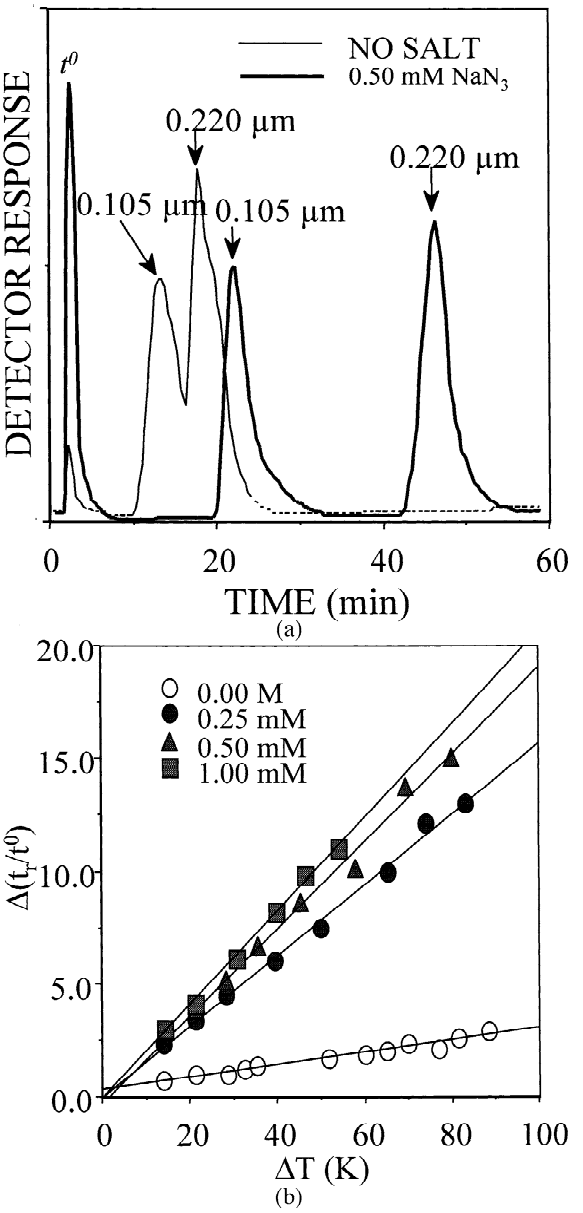

Fig. 7. (a) Superimposed fractograms of a mixture of 0.105- and 0.220-μm PS latex particles in aqueous carrier solution made up of 0.1% FL-70 surfactant in the absence and presence of 0.50 m*M* concentration of NaN_3 (bold-solid line). Experimental conditions: flow-rate = 0.30 ml/min, $\Delta T = 45$ K and $w = 76$ μm. (b) Plots of $\Delta(t_r/t^0)$ versus concentration of TBAP in ACN carrier liquid obtained under different conditions of ΔT. $\Delta(t_r/t^0)$ is defined as the difference between t_r/t^0 for the 0.105- and 0.220-μm PS particles. Experimental conditions: flow-rate = 0.30 ml/min, $T_c = 298$ K and $w = 76$ μm.

of $\Delta(t_r/t^0)$ (defined as the difference between t_r/t^0 for the 0.105- and 0.220-μm PS particles) versus TBAP concentration under different ΔT conditions. The figure shows linear variations in $\Delta(t_r/t^0)$ with ΔT at various concentrations of TBAP, demonstrating the influence of TBAP concentration on not only improved particle retention times but also separation resolution. The tunability of resolution as a function of electrolyte concentration at modest field strengths is also illustrated. The combined effect of field strength and electrolyte concentration affords the technique of ThFFF greater flexibility to achieving the desired level of retention and resolution. One example is the possibility of achieving an adequate level of particle retention with a correspondingly low ΔT but with a higher TBAP concentration instead of always relying on higher ΔT conditions to achieve the same level of particle retention times.

In view of the observation that higher electrolyte concentrations result in improved resolution between particles of different sizes, it is expected that the same conclusion can be drawn from experimentally determined diameter-based selectivity, S_d values obtained under different electrolyte concentrations. (That is, S_d values should increase with increases in electrolyte concentration since S_d is a measure of the ability of the system to differentially retain and thus resolve particles of different sizes.) Fig. 8 shows plots of log (t_r/t^0) versus log d obtained using retention data from Fig. 6. These plots illustrate differences in S_d values among carriers containing different NaCl concentrations. According to Eq. (7), the slope of each plot is equal to the S_d for the electrolyte concentration represented by that plot. From the figure, it is clear that the S_d values of 1.50, 1.42, 1.23, 1.18, 0.97, and 0.87 corresponding to NaCl concentrations of 0.50, 1.0, 3.0, 6.0, 50.0, and 100.0 m*M*, respectively, seem to decrease with increasing NaCl concentration. This rather anomalous behavior is being reported here for the first time. Jeon et al. [25] reported only a slight reduction in S_d value from 1.6 to 1.5 for PS particles in 3 m*M* and 9 m*M* NaN_3, respectively, contained in a 0.1% FL-70 aqueous medium. Mes et al. [27] reported a low S_d value of 0.54 for PS particles when water containing 0.5 m*M* TBAP and 1.0 m*M* sodium dodecyl sulfate (SDS) was used as carrier and much higher selectivities of 1.30 and 1.45 for PS particles

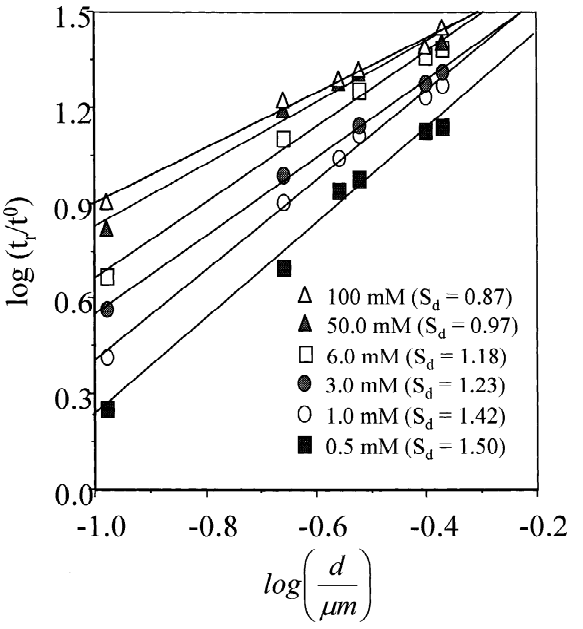

Fig. 8. Logarithmic plot of retention time t_r (relative to void time t^0) versus particle diameter d (0.105, 0.220, 0.280, 0.300, 0.398 and 0.426 μm) for the various retention measurements of Fig. 6 obtained under different NaCl concentrations in aqueous media. The NaCl concentration corresponding to higher plots provides higher thermal diffusivity values. The slope of the plot represents the diameter-based selectivity S_d for each concentration represented.

with ACN–water carrier mixtures of composition 5 and 10% (mol/mol), respectively. Both the ACN–water carrier mixtures contained 0.5 m*M* TBAP and 1 m*M* SDS. They however, never reported any influence of varying quantities of TBAP on size-based selectivity. Liu et al. [20] on the other hand, only reported the variation in S_d with differences in chemical composition of the particles. (They reported values of S_d in the vicinity of 1.5 for latexes and 1.33 for silica and postulated that D_T could be increasing approximately with $d^{0.5}$.) Our results however, indicate that the exponent of d varies depending on the ionic strength and/or chemical composition of the carrier solution. For instance, from the plots of log (t_r/t^0) versus log d for PS in ACN (omitted here for reasons of brevity), the S_d values of 1.50, 1.40, and 0.96 corresponding to the much lower TBAP concentrations of 0.005, 0.01, and 0.05 m*M*, respectively, are quite comparable to those

found with the aqueous carriers. At first glance, these results appear to contradict the revelation that higher electrolyte concentrations improve resolution as is evident from Fig. 7a,b. Upon further examination, the results of Fig. 7a indicate a marked improvement in the resolution between the 0.105- and 0.220-μm PS latex particles at higher NaN_3 concentration.

Critical examination of the results of Fig. 6 reveal that despite the relatively larger increases in NaCl concentration, the corresponding changes in t_r/t^0 with diameter are rather subtle with increasing NaCl concentration. It is apparent that the trend in S_d values with NaCl concentration is a more complex retention-diameter-electrolyte related phenomenon (see Section 4.1). Clearly, more work is needed to determine the exact nature of the influence of various salt concentrations on D_T. The results of the variations in S_d with TBAP concentration in ACN however, further reinforces previous findings by several authors that ACN carrier solution affords longer retention times for particulate material in ThFFF [22,25–27].

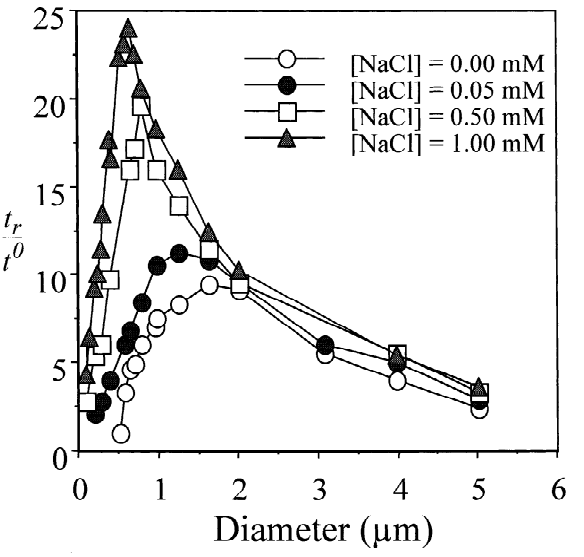

Fig. 9. Plots of t_r/t^0 versus PS particle diameters (0.105, 0.220, 0.280, 0.300, 0.398, 0.426, 0.598, 1.05, 1.48, 1.75, 2.08, 3.00, 3.98 and 5.01 μm) obtained under various concentrations of NaCl in a 0.1% FL-70 aqueous carrier solution. Experimental conditions: flow-rate = 0.30 ml/min, ΔT = 60 K, T_c = 288 K and w = 114 μm.

4.1. Effect of ionic strength on steric inversion diameter

The retention inversion phenomenon in FFF represents one of the most serious complications in the theoretical treatment and practical implementation of the conceptually simple FFF family of techniques [42]. In this phenomenon, retention time (t_r) increases monotonically with particle diameter up to a maximum after which it begins a long descent with further increases in particle diameter. This phenomenon can complicate particle size analysis for particle populations with diameters that span the inversion diameter. Successful particle size analysis requires that each retention time element be associated with a specific diameter. However, because of inversion phenomenon, each value of t_r specifies two values of diameter [42]. Since ionic strength will determine the distance of closest approach of a particle to the accumulation wall, we decided to investigate the effect of electrolyte concentration on the steric inversion diameter, d_i. Fig. 9 shows plots of t_r/t^0 versus PS particle diameter for different concentrations of NaCl in a 0.1% FL-70 aqueous carrier solution. There is a general shift in d_i from 1.60 to 1.20, 0.80, and 0.60 μm when the concentration of NaCl is increased from 0.00 to 0.05, 0.50, and 1.00 m*M*, respectively. Thus, ionic strength provides us the additional flexibility to shift up or down the value of d_i and to the best of our knowledge, it is the first report of its kind.

Additional experiments with ACN not only yielded lower d_i values, but also a reversal in the order of the shift in d_i from 0.300 to 0.325, 0.400 and 0.500 μm when the concentration of TBAP increased from 0.00 to 0.01, 0.05, and 0.10 m*M*, respectively. (These results are however omitted for reasons of brevity.) An explanation for this difference in behavior between the two carrier types is presently not available, but the observation reinforces the previously reported differences in particle retention behavior between these carrier solutions [22]. Further investigation is needed.

4.2. Effect of ionic strength on sample recovery

The recoveries of a known quantity of 0.220-μm PS latex beads were determined under three different concentrations of NaCl and various ΔT conditions in

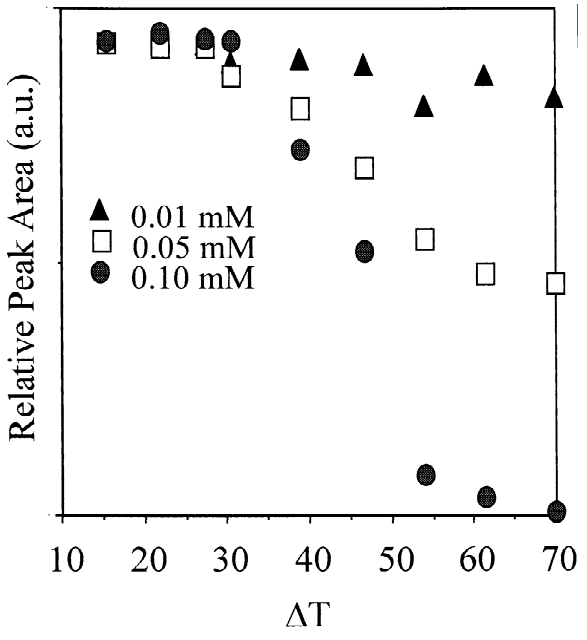

Fig. 10. Plots of relative peak area of 0.220-μm PS versus ΔT obtained under different conditions of NaCl concentrations in an aqueous carrier solution. Experimental conditions: flow-rate = 0.30 ml/min, $T_c = 298$ K and $w = 76$ μm.

an aqueous carrier by calculating the elution peak areas (Fig. 10). The peak areas corresponding to NaCl concentrations of 0.05 and 0.10 m*M* remained constant over the ΔT range of 15 to about 30 K. (Peak area data for 0.01 m*M* NaCl are missing over the cited ΔT range due to incomplete resolution of the peaks from the void peak.) Beyond $\Delta T = 30$ K, the peak areas corresponding to NaCl concentrations of 0.05 and 0.10 m*M* reduced monotonically with increases in ΔT. The rate of reduction was much greater for the highest NaCl concentration with the peak area reduced to almost zero at $\Delta T = 70$ K. The higher rates of reduction in peak areas with increases in both ΔT and NaCl concentration are not surprising. Higher values of both ΔT and NaCl concentration promote the closest approach of the particles to the accumulation wall and hence a greater chance of particle adsorption onto the channel surface. Hence the reduction in peak areas. This implies that for adequate retention, peak resolution and sample recovery, optimum conditions of ΔT and electrolyte concentration must be selected.

5. Conclusions

Modification of the ionic strength of an aqueous or non-aqueous carrier solution can have profound effects on particle retention behavior in a ThFFF system. These effects can be either beneficial or otherwise, depending on the performance criteria under consideration. For instance, whereas we can achieve improved resolution with higher electrolyte concentrations, such conditions may lead to greater sample loss through adsorption onto the channel accumulation wall. This is particularly serious when higher ΔT conditions are also employed. Thus, there has to be a balance between electrolyte concentration and the ΔT conditions. The effects are more pronounced with aqueous carriers where minimal or total lack of particle retention is often observed in the absence of an electrolyte irrespective of practical ΔT-values employed. In general, higher electrolyte concentrations not only yield longer retention times but also provide better resolution. A significant advantage of this effect is that it is possible to achieve desirable particle retention times with lower ΔT conditions resulting in lower energy consumption. There is however, a limit as to how much electrolyte can be added to a given carrier solution under specific ΔT conditions. Adsorptive sample loss on the channel surface increases with higher electrolyte concentrations and particularly when larger ΔT conditions are employed.

6. Nomenclature

d	particle diameter, μm
D	ordinary diffusion coefficient, $m^2\ s^{-1}$
D_T	thermal diffusion coefficient, $m^2\ s^{-1}\ K^{-1}$
k	Boltzmann's constant, $J\ K^{-1}$
l	mean layer thickness of sample cloud, μm
R	retention ratio
S_d	diameter-based selectivity
t_r	retention time
t^0	channel void time
T	temperature, K
T_c	cold wall temperature, K
w	channel thickness, μm
ΔT	temperature drop applied across channel

η carrier viscosity, Pa s
λ dimensionless retention parameter

Acknowledgements

This work was supported in part by Grant 96-116RG/CHE/AF/AC from the Third World Academy of Sciences (TWAS). S.M.M. acknowledges support from the German Academic Exchange Services (DAAD) for the award of a scholarship in support of his graduate school program.

References

[1] J.C. Giddings, Science 260 (1993) 1456.
[2] J. Janca, Field-Flow Fractionation, Marcel Decker, New York, 1987.
[3] K.D. Caldwell, in: H.G. Barth (Ed.), Modern Methods of Particle Size Analysis, Wiley, New York, 1984, Chapter 7.
[4] J.C. Giddings, F.J.F. Yang, M.N. Myers, Sep. Sci. 10 (1975) 133.
[5] J.C. Giddings, G. Karaiskakis, K.D. Caldwell, M.N. Myers, J. Colloid Interface Sci. 92 (1983) 66.
[6] M.E. Schimpf, J. Chromatogr. 517 (1990) 405.
[7] G.H. Thompson, M.N. Myers, J.C. Giddings, Sep. Sci. 2 (1967) 797.
[8] J.C. Giddings, M.E. Hovingh, G.H. Thompson, J. Phys. Chem. 74 (1970) 4291.
[9] M. Martin, P. Reynaud, Anal. Chem. 52 (1980) 2293.
[10] J. Janca, K. Kleparnik, Sep. Sci. Technol. 16 (1981) 657.
[11] M. Martin, J. Hes, Sep. Sci. Technol. 19 (1984) 685.
[12] J.J. Kirkland, S.W. Rementer, W.W. Yau, J. Appl. Polym. Sci. 38 (1989) 1383.
[13] M.E. Schimpf, J. Chromatogr. 517 (1990) 405.
[14] Y. Gao, X. Chen, J. Appl. Polym. Sci. 45 (1992) 887.
[15] J.J. Kirkland, S.W. Rementer, Anal. Chem. 64 (1992) 904.
[16] A.C. van Asten, E. Venema, W.Th. Kok, H. Poppe, J. Chromatogr. 644 (1993) 83.
[17] J.J. Gunderson, J.C. Giddings, Macromolecules 19 (1986) 2618.
[18] M.E. Schimpf, J.C. Giddings, J. Polym. Sci. Polym. Phys. Ed. 27 (1989) 1317.
[19] M.E. Schimpf, J.C. Giddings, Macromolecules 20 (1987) 1561.
[20] G. Liu, J.C. Giddings, Chromatographia 34 (1992) 483.
[21] G. Liu, J.C. Giddings, Anal. Chem. 63 (1991) 296.
[22] P.M. Shiundu, G. Liu, J.C. Giddings, Anal. Chem. 67 (1995) 2705.
[23] P.M. Shiundu, J.C. Giddings, J. Chromatogr. A 715 (1995) 117.
[24] S.K. Ratanathanawongs, P.M. Shiundu, J.C. Giddings, Colloids Surf. A 105 (1995) 243.
[25] S.J. Jeon, M.E. Schimpf, A. Nyborg, Anal. Chem. 69 (1997) 3442.
[26] S.J. Jeon, M.E. Schimpf, in: T. Provder (Ed.), Particle Size Distribution III: Assessment and Characterization, American Chemical Society Symposium Series No. 693, ACS, Washington, DC, 1998, Chapter 13, pp. 182–195.
[27] E.P.C. Mes, R. Tijssen, W.Th. Kok, J. Chromatogr. A 907 (2001) 201.
[28] J.C. Giddings, Science 69 (1997) 552.
[29] M.E. Hansen, J.C. Giddings, Anal. Chem. 61 (1989) 811.
[30] M.E. Hansen, J.C. Giddings, R. Becket, J. Colloid Interface Sci. 132 (1989) 300.
[31] Y. Mori, K. Kimura, M. Tanigaki, Anal. Chem. 62 (1990) 2668.
[32] T. Hoshino, M. Suzuki, K. Ysukawa, M. Takeuchi, J. Chromatogr. 400 (1987) 361.
[33] M. Takeuchi, T. Saito, T. Hoshino, in: Proceedings of Chromatography International Symposium, The Division of Liquid Chromatography of the Japan Society for Analytical Chemistry, Tokyo, Japan, 1989, p. 711.
[34] M.E. Schimpf, S.N. Semenov, J. Phys. Chem. B 105 (2001) 2285.
[35] S.N. Semenov, J. Microcol. Sep. 9 (4) (1997) 287.
[36] M.N. Myers, J.C. Giddings, Anal. Chem. 54 (1982) 2284.
[37] J.C. Giddings, in: Unified Separation Science, Wiley, New York, 1991.
[38] A.C. van Asten, H.F.M. Boelens, W.Th. Kok, H. Poppe, P.S. Williams, J.C. Giddings, Sep. Sci. Technol. 29 (1994) 513.
[39] M.E. Schimpf, Trends Polym. Sci. 4 (1996) 114.
[40] J.C. Giddings, P.M. Shiundu, S.M. Semenov, J. Colloid Interface Sci. 176 (1995) 454.
[41] P.S. Williams, Y. Xu, P. Reschiglian, J.C. Giddings, Anal. Chem. 69 (1997) 349.
[42] J.C. Giddings, Analyst 118 (1993) 1487.